COMPUTING SHOCK WAVES IN CLOUD CAVITATION

Christopher E. Brennen, Tim Colonius and Fabrizio d'Auria
California Institute of Technology
Mail Code 104-44, Pasadena, CA 91125

ABSTRACT

This paper presents a numerical investigation of some of the phenomena involved in the nonlinear dynamics of a homogeneous bubbly mixture bounded by an oscillatory wall. This problem represents an idealization of the flow in a typical vibratory cavitation damage device. Results are presented showing that wave steepening and ultimately shock wave formation occur as the magnitude of the excitation increases. The propagation characteristics of the waves through the bubbly medium have also been studied. Strong pressure peaks of short duration, corresponding to the coherent collapse of the bubble clusters, are computed and accurately resolved, both in space and time. As the amplitude of the excitation is increased a series of period doubling bifurcations occurs. The nonlinear dynamics of the oscillating bubble cluster are observed to follow a subharmonic route to chaos.

1. INTRODUCTION

The collapse of a cluster of bubbles in close proximity to each other, commonly referred to as cloud cavitation, is responsible for severe cavitation noise and damage. The destructive effects associated with the growth and collapse of cloud cavitation have received considerable attention (Knapp [1], Bark and van Berlekom [2], Soyama et al. [3]) and are still the object of intensive research (Reisman et al. [4]). The experimental observations of cloud cavitation (for example, Wade and Acosta [5], Kubota et al. [6], Le et al. [7], de Lange et al. [8]) consistently show that the radiated noise produced by cloud cavitation is characterized by very strong pressure peaks of short duration.

A few analytical efforts have addressed the same issues. Hansson and Mørch [9] were among the first to suggest that the concerted collapse of a cluster of bubbles involves the creation of an inwardly propagating shock wave. They also suggested that the focusing of the shock at the center of the cloud was responsible for the enhancement of cavitation noise and damage. Experimental observations by Lauterborn et al. [10] show strong interactions between single bubbles and give evidence of a 'highly cooperative system'. Smereka and Banerjee [11] studied the chaotic motion of a cloud of bubbles. Wang and Brennen ([12], [13]) have studied the nonlinear growth and collapse of a bubble cloud and their computations show that geometric focusing may lead to very large local pressures.

In this paper we study the nonlinear dynamics of a cloud of bubbles bounded by a single, plane oscillating wall. This one-dimensional analysis may be regarded as an idealization of a vibratory cavitation damage device (Knapp et al. [14]). Details of the numerical scheme have been presented elsewhere (Colonius et al. [15]) and this paper will focus on the physical phenomena manifest by the calculations. Violent pressure peaks result from the periodic cloud collapse

and the dependence of the pressure perturbations on the flow parameters is analyzed. Moreover, depending on the frequency and amplitude of the wall motion, the dynamics of a bubble cloud follow a subharmonic route to chaos.

2. GOVERNING EQUATIONS AND NUMERICAL APPROACH

The continuum equations governing the flow of a homogeneous bubbly mixture (d'Agostino and Brennen [16], Biesheuvel and van Wijngaarden [17]) have been discussed in detail elsewhere (d'Agostino and Brennen [18], Brennen [19]) and the present numerical method is discussed in Colonius et al. [15].

Neglecting the contributions of gravity and viscosity, the continuity and momentum equations for the bubbly mixture are:

$$\frac{D\rho}{Dt} + \rho\frac{\partial u_i}{\partial x_i} = 0, \tag{1}$$

$$\frac{Du_j}{Dt} + \frac{1}{\rho}\frac{\partial p}{\partial x_j} = 0. \tag{2}$$

where ρ is the mixture density, p is the pressure in the liquid, u_i is the mixture velocity, x_i is a spatial coordinate and t is the time. The mixture density is made dimensionless by the constant liquid density, ρ_L, the lengths, x_i, and the bubble radius, R, are normalized by an equilibrium bubble radius R_0, the mixture velocity, u_i, is normalized by the bubble natural frequency, ω_0 times the equilibrium bubble radius, the pressure, P is measured relative to its equilibrium value, p_0, and normalized by $\rho_L r_0^2\omega_0^2$. Time, t, is normalized by $1/\omega_0$. The bubble radius $R(x_i,t)$ is related to the pressure in the mixture by the Rayleigh-Plesset equation:

$$\begin{aligned} R\frac{D^2R}{Dt^2} &+ \frac{3}{2}\left(\frac{DR}{Dt}\right)^2 + \delta_D\frac{1}{R}\frac{DR}{Dt} \\ &+ \frac{2}{\mathrm{We}}\left(R^{-1} - R^{-3\gamma}\right) \\ &+ \frac{\sigma}{2}\left(1 - R^{-3\gamma}\right) + P = 0, \end{aligned} \tag{3}$$

where We is the Weber number, σ is the cavitation number, γ is the ratio of specific heats and δ_D is the damping coefficient in the bubble dynamics which is discussed later. The mixture density, ρ, and the bubble radius, R, are related as follows:

$$\rho = \left(1 + \frac{\alpha_0 R^3}{1-\alpha_0}\right)^{-1} \tag{4}$$

where α_0 is the initial void fraction of the mixture.

As discussed in Colonius et al. [15], a major issue in the numerical analysis of the nonlinear dynamics of the bubbly mixture is the choice of the magnitude of the damping coefficient δ_D, (van Wijngaarden [20]). This choice must not only provide a realistic description of the phenomena involved in the dynamics of the bubble cloud (amount of growth, violence of the collapse, number of rebounds, etc.) but must insure sufficient numerical resolution. Colonius et al. [15] have shown that there exists a threshold value below which the computational effort required to obtain sufficient resolution (both in space and time) increases significantly. Below this threshold, the main effect of decreased damping is a greater number of rebounds after the bubble collapse. A value of δ_D of the order of 1 is often necessary to match the theoretical predictions with the experimental results (van Wijngaarden [20]) and values in this range are used in the present study ($0.4 \leq \delta_D \leq 8$).

Colonius et al. [15] describe the one-dimensional implicit Lagrangian finite volume scheme which is also employed here. The choice of an implicit scheme was dictated by the necessity of discretely conserving both mass and momentum. Also, it has the advantage of efficiently handling the inherent stiffness of the system of equations (1), (2), and (3). A Richardson extrapolation technique (Hairer and Wanner [21]) based on the implicit Euler scheme was implemented and validated.

3. RESULTS AND DISCUSSION

We consider the one-dimensional flow of a bubbly mixture bounded by a single, plane wall oscillating normal to itself (Figure 1). The component of the mixture velocity normal to the wall is equal to the wall velocity:

$$u_w(x_w,t) = A\sin(2\pi\omega t) \tag{5}$$

At the other end of the finite computational domain a nonreflecting boundary condition is imposed, as discussed by Colonius et al. [15]. The three parame-

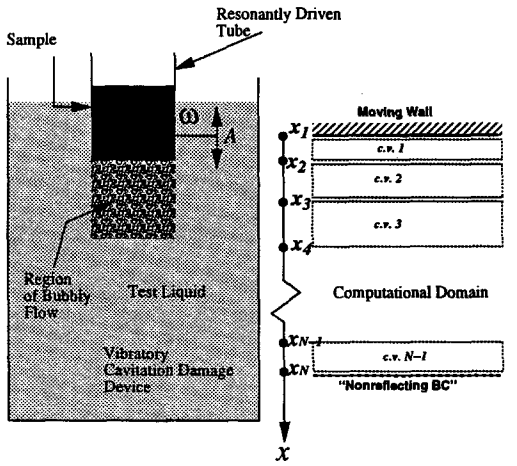

Figure 1: Schematic diagram of the vibratory cavitation device (left) and of the corresponding computational domain.

ters governing the flow are the period of oscillation of the wall, T ($T = 2\pi/\omega$), the amplitude A, and the damping parameter, δ_D. Three different flow regimes are investigated, namely subresonant, resonant and super-resonant (d'Agostino et al. [22]); note that resonant conditions are given by $\omega = 1$ as a result of the normalization. The initial void fraction in the bubbly mixture has been varied in the range $2.5 \times 10^{-4} \leq \alpha_0 \leq 10^{-2}$.

We first focus on the subresonant case. If the amplitude of oscillation of the wall is sufficiently small, only linear acoustic waves are observed. The waves propagate through the domain with real phase speed (see Colonius et al. [15]) and with only slight attenuation due to the damping term. As the amplitude is increased nonlinear effects occur; shock waves are generated at the moving wall and propagate through the domain near the wall. Bubbles experience larger and larger growth and their subsequent collapse becomes more violent. This is exemplified in Figure 2, which shows the behavior of the pressure and bubble

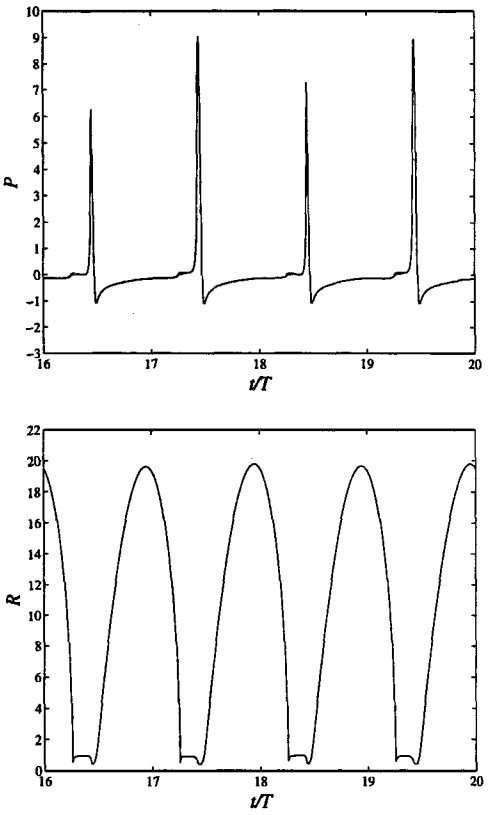

Figure 2: Subresonant regime. Nondimensional pressure and radius at the wall as a function of time, $16 \leq t/T \leq 20$, for $\omega = 0.03$, $A = 0.4$, $\delta_D = 2$, and $\alpha_0 = 2.5 \times 10^{-4}$.

radius at the wall as a function of time. The pressure manifests violent spikes corresponding to each cloud collapse at the wall. It is important to notice that the periodicity of the collapse is the same as that of the wall motion.

Colonius et al. [15] considered the effect of the damping parameter, δ_D, on the growth and collapse near the wall. For a given amplitude, A, there appears to be a value of δ_D above which the growth and maximum size of the bubble are attenuated. Below this critical value, the primary effect of δ_D is to

reduce the number of rebounds after collapse. Note that in the present case we choose δ_D high enough so that only a single rebound is present after each collapse. Moreover, a large number of cycles are necessary for the computation to achieve a steady state and this number increases with the amplitude, A.

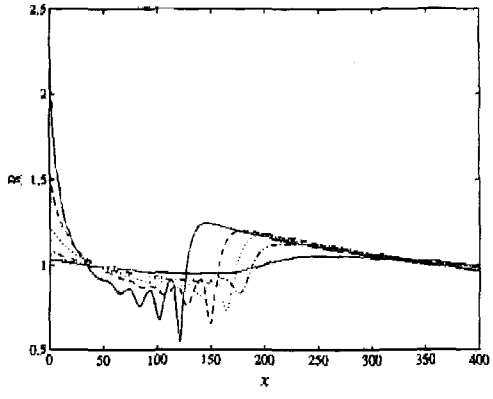

Figure 3: Behavior of the bubble radius in space, at time $t/T = 76$, for $A = 0.01$ (——), $A = 0.025$ (—·—), $A = 0.05$ (·····), and $A = 0.1$ (----), and $A = 0.3$ (——). In all cases $\omega = 0.1$, $\delta_D = 0.1$, and $\alpha_0 = 10^{-2}$.

As the wall motion is increased, the amplitude of the generated shock wave saturates and increased bubble growth occurs only in a very thin layer near the wall. This spatial behavior is depicted in Figure 3. Note that for $A = 0.01$ the small variation in bubble radius with distance x is approximately sinusoidal. As the amplitude increases, the wave steepens into a shock. The shock strength eventually saturates and a very thin boundary layer is formed, above which the wall motion is essentially 'cut-off'. The situation is similar to the one described for bubble clouds by Smereka and Banerjee [11] and can be understood in terms of a cut-off frequency beyond which acoustic waves no longer have real phase speed, but are exponentially damped with increasing distance from the wall. This follows from the greatly reduced bubble natural frequency in the region where the explosive bubble growth takes place. The flow is no longer locally subresonant in the thin layer near the wall.

At resonance, the linear phase speed, given by:

$$c = \omega/k = \pm\left(\frac{1}{3\alpha_0(1-\alpha_0)}\left(1-\omega^2-i\omega\delta_D\right)\right)^{\frac{1}{2}} \quad (6)$$

is complex and proportional to the square root of the frequency and the damping. Thus for low amplitude (the linear case), the waves are exponentially damped with increasing distance from the wall. For higher amplitudes, a period doubling in the response of the bubble layer near the wall occurs: the emergence of the subharmonic frequency means that the motion is no longer completely cut-off, but a portion of energy propagates away from the wall. A typical example of the pressure and radius at the wall are shown in Figure 4 and Figure 5 for a few cycles of the wall oscillation. A similar period doubling route to chaos was also detected in the bubble cloud calculations of Smereka and Banerjee [11].

Figure 5 shows that very strong pressure peaks can occur at resonant conditions, even for moderate amplitudes (when compared to the sub-resonant case in Figure 2). Insuring accurate resolution (both in space and time) of pressure peaks such as those shown in Figure 5 represents a major effort in the present numerical study. While time resolution is automatically obtained in the present scheme, a correct description of the pressure in space is only obtained using a sufficiently refined mesh.

Figure 6 is a bifurcation diagram showing the behavior of the bubble radius in the cloud as a function of the wall motion, for a given frequency of oscillation. It illustrates a typical period-doubling route to chaos. As the amplitude of the wall motion is increased, the bubble radius undergoes a series of bifurcations eventually leading to a chaotic attractor.

The results presented here for a bubble cloud show certain similarities to the nonlinear dynamics of individual bubbles (Lauterborn and Parlitz [23]) and bubble clouds (Smereka and Banerjee [11]). For example, the occurrence of period doublings and cascades to chaos are observed in resonance studies of single bubbles treated as nonlinear oscillators (Feng

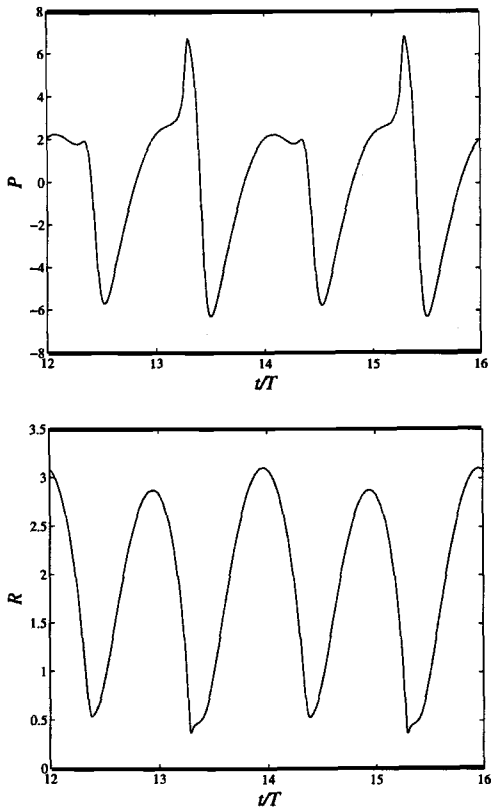

Figure 4: Resonant regime. Nondimensional pressure and radius at the wall as a function of time, $12 \leq t/T \leq 16$, for $\omega = 1$, $A = 0.1$, $\delta_D = 4$, and $\alpha_0 = 2.5 \times 10^{-4}$. Period doubling results in a stronger collapse every other cycle.

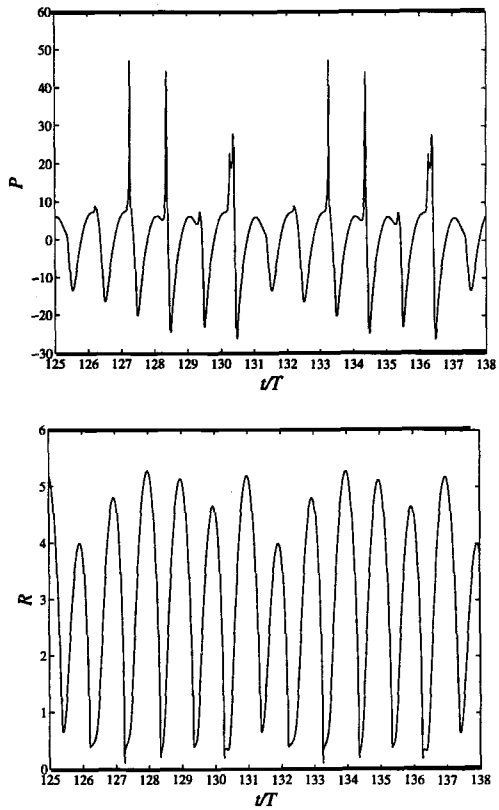

Figure 5: Resonant regime. Nondimensional pressure and radius at the wall as a function of time, $125 \leq t/T \leq 138$, for $\omega = 1$, $A = 0.35$, $\delta_D = 8$, and $\alpha_0 = 2.5 \times 10^{-4}$. A strong cloud collapse occurs every six oscillation cycles.

and Leal [24]). Furthermore, Lauterborn and Koch [25], and Lauterborn et al. [10] have experimentally observed that a bubble cloud under ultrasound will follow a subharmonic route to chaos with a low dimensional strange attractor. In their earlier experiments on a vibratory cavitation device, Hansson and Mørch [9] also observed that, depending on the experimental parameters, total collapse of the bubbly mixture was not achieved in each cycle but could stretch over two or more cycles. The present results give a further explanation of these experimental observations.

Period doubling leading to chaos also occurs at super-resonant conditions. A typical example of the transition to chaotic behavior is shown in Figure 7 and 8. The phase diagram of Figure 8, clearly shows the absence of a periodic structure and the transition towards a chaotic behavior.

4. CONCLUSIONS

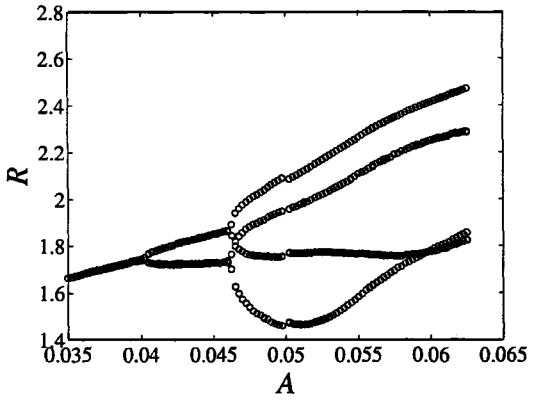

Figure 6: Bifurcation diagram. The radius, R is plotted as a function of the amplitude, A, for $\omega = 1$, $\delta_D = 0.4$, and $\alpha_0 = 10^{-2}$.

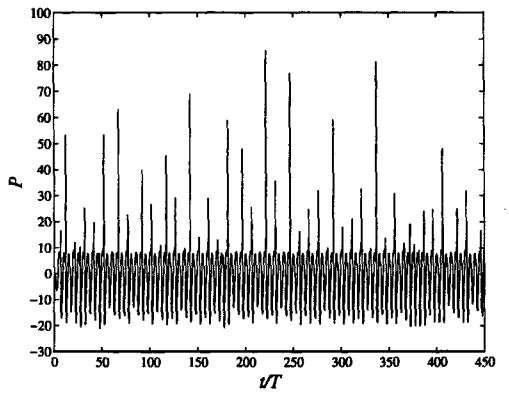

Figure 7: Super-Resonant regime. Nondimensional pressure at the wall as a function of time, $0 \leq t/T \leq 450$, for $\omega = 2$, $A = 0.175$, $\delta_D = 8$, and $\alpha_0 = 2.5 \times 10^{-4}$.

The one-dimensional flow of a bubbly mixture in an idealized vibratory cavitation device has been studied. The nonlinear dynamics of the bubbly mixture have been analyzed for subresonant, resonant and super-resonant regimes. As the wall motion increases

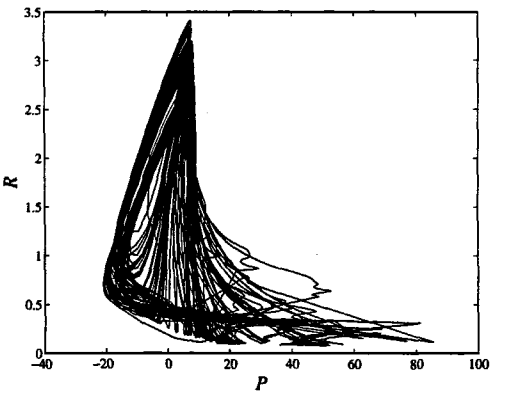

Figure 8: Super-Resonant regime. Phase diagram illustrating the transition towards a chaotic behavior in time of the radius and pressure; $0 \leq t/T \leq 450$, for $\omega = 2$, $A = 0.175$, $\delta_D = 8$, and $\alpha_0 = 2.5 \times 10^{-4}$.

in amplitude, strong shock waves form at the wall and propagate through the mixture. The numerical scheme accurately resolves the shock waves and associated violent bubble collapses and strong pressure pulses.

Analysis of the wave propagation in the domain shows that, as the amplitude of the wall motion is increased above a critical value, saturation occurs in the strength of the shock waves. Also, as the growth and collapse of the bubble become more violent, the shocks are confined to a small region close to the oscillating surface.

In the subresonant regime no period doubling was observed in the bubble collapse. In the resonant and super-resonant regimes period doubling was observed, as the amplitude of the wall motion was increased. Ultimately, the nonlinear dynamics of the bubbly mixture follow a subharmonic route to chaos.

ACKNOWLEDGEMENTS

This research was supported, in part, by the Office of Naval Research under grant number N00014-91-J-1295. The third author is also grateful for support from the European Space Agency.

REFERENCES

[1] R.T. Knapp. Investigations of the mechanics of cavitation and cavitation damage. *Trans ASME*, 77:1045–1054, 1955.

[2] G. Bark and L. von Berlekom. Experimental investigations of cavitation noise. In *Proc. 12th ONR Symp. on Naval Hydrodynamics*, pages 301–318. ASME, 1978.

[3] H. Soyama, Kato H., and R. Oba. Cavitation observations of severely erosive vortex cavitation arising in a centrifugal pump. In *Proc. 3rd IMechE Intl Conf. on Cavitation*, pages 103–110. 1992.

[4] G. Reisman, Y.-C. Wang, and C.E. Brennen. Observation of shock waves in cloud cavitation. to be appear in the *J. Fluid Mech.*, 1998.

[5] R.B. Wade and A.J. Acosta. Experimental observation on the flow past a plano-convex hydrofoil. *ASME J. Basic Eng*, 88:273–283, 1966.

[6] A. Kubota, H. Yamaguchi, and M. Maeda. Unsteady structure measurement of cloud cavitation on a foil section using conditional sampling. *ASME J. Fluids Eng.*, 111:204–210, 1989.

[7] Q. Le, J.M. Franc, and J.M. Michel. Partial cavities: global behavior and mean pressure distribution. *ASME J. Fluids Eng*, 115:243–248, 1993.

[8] D.F. de Lange, G.J. de Bruin, and L. van Wijngaarden. On the mechanism of cloud cavitation-experiment and modeling. In *Proc. 2nd Symp. on Cavitation, Tokyo*, pages 45–50. 1994.

[9] I. Hansson and K.A. Mørch. The dynamics of cavity clusters in ultrasonic (vibratory) cavitation erosion. *J. Appl. Phys.*, 51:4651–4658, 1980.

[10] W. Lauterborn, E. Schmitz, and A. Judt. Experimental approach to a complex acoustic system. *Int. J. Bifurcation Chaos*, 3:635–642, 1993.

[11] P. Smereka and S. Banerjee. The dynamics of periodically driven bubble clouds. *Phys. Fluids*, 31:3519–3531, 1988.

[12] Y.-C Wang and C.E Brennen. Shock wave development on the collapse of a cloud of bubbles. In *Cavitation and Multiphase Flow Forum*, volume FED 194, page 15. ASME, 1994.

[13] Y.-C Wang and C.E Brennen. The noise generated by the collapse of a cloud of cavitation bubbles. In *ASME/JSME Symposium on Cavitation and Gas-Liquid Flow in Fluid Machinery and Devices*, volume FED 226, page 17. ASME, 1995.

[14] R.T. Knapp, J.W. Daily, and F.G. Hammitt. *Cavitation*. McGraw-Hill, 1970.

[15] T. Colonius, C.E Brennen, and F. d'Auria. Computations of shock waves in cavitating flow. In *ASME Fluids Engineering Summer Meeting*. 1998.

[16] L. d'Agostino and C.E. Brennen. On the acoustical dynamics of bubble clouds. In *ASME Cavitation and Multiphase Flow Forum*, pages 72–75. 1983.

[17] A. Biesheuvel and L. van Wijngaarden. Two phase flow equations for a dilute dispersion of gas bubbles in liquid. *J. Fluid Mech.*, 148:301–318, 1984.

[18] L. d'Agostino and C.E. Brennen. Linearized dynamics of spherical bubble clouds. *J. Fluid Mech.*, 199:155–176, 1989.

[19] C.E. Brennen. *Cavitation and Bubble Dynamics*. Oxford University Press, 1995.

[20] L. van Wijngaarden. One-dimensional flow of liquids containing small gas bubbles. *Ann. Rev. Fluid Mech.*, 4:369–396, 1972.

[21] E. Hairer and G. Wanner. *Solving Ordinary Differential Equations II*. Springer, rev edition, 1996.

[22] L. d'Agostino, C.E. Brennen, and A.J. Acosta. Linearized dynamics of two-dimensional bubbly and cavitating flows over slender surfaces. *J. Fluid Mech.*, 192:485–509, 1988.

[23] W. Lauterborn and U. Parlitz. Methods of chaos physics and their application to acoustics. *J. Acoust. Soc. Am.*, 84:1975–1993, 1988.

[24] Z.C. Feng and L.G. Leal. Nonlinear bubble dynamics. *Ann. Rev. Fluid Mech.*, 29:201–243, 1997.

[25] W. Lauterborn and A. Koch. Holographic observation of period doubled and chaotic bubble oscillations in acoustic cavitation. *Phys. Rev.*, 35:1974–1976, 1987.